Cytotoxic, antimicrobial and antiviral secondary metabolites produced by the plant pathogenic fungus *Cytospora* sp. CCTU A309

Abolfazl Narmani[a,b], Rémy Bertrand Teponno[a,c], Mahdi Arzanlou[b], Frank Surup[a], Soleiman E. Helaly[a,d], Kathrin Wittstein[a], Dimas F. Praditya[e,f], Asadollah Babai-Ahari[b], Eike Steinmann[e], Marc Stadler[a,*]

[a] *Department of Microbial Drugs, Helmholtz Centre for Infection Research and German Centre for Infection Research (DZIF), partner site Hannover/Braunschweig, Inhoffenstrasse 7, 38124 Braunschweig, Germany*
[b] *Department of Plant Protection, Faculty of Agriculture, University of Tabriz, Tabriz, Iran*
[c] *Department of Chemistry, Faculty of Science, University of Dschang, P.O. Box 67, Dschang, Cameroon*
[d] *Department of Chemistry, Faculty of Science, Aswan University, 81528 Aswan, Egypt*
[e] *Department of Molecular and Medical Virology, Ruhr-University Bochum, 44801 Bochum, Germany*
[f] *Research Center for Biotechnology, Indonesian Institute of Science, Jl. Raya Bogor KM 46, Cibinong, Indonesia*

* Correspondence: marc.stadler@helmholtz-hzi.de ; Tel.: +49 531 6181-4240; Fax: +49 531 6181 9499

Abstract

Chemical analysis of extracts from cultures of the plant pathogenic fungus *Cytospora* sp. strain CCTU A309 collected in Iran led to the isolation of two previously unreported heptanedioic acid derivatives namely (2*R*,3*S*) 2-hydroxy-3-phenyl-4-oxoheptanedioic acid (**1**) and (2*S*,3*S*) 2-hydroxy-3-phenyl-4-oxoheptanedioic acid (**2**) as diastereomers, four previously undescribed prenylated *p*-terphenyl quinones **3-6** in addition to five known metabolites. Their structures were elucidated on the basis of extensive spectroscopic analysis and high-resolution mass spectrometry. While the relative configurations of **1** and **2** were reasoned by a *J*-based analysis and confirmed by comparison of ^{13}C chemical shifts to literature data, their absolute configurations were deduced from comparison of the ^{1}H NMR difference of their (*S*)- and (*R*)-phenylglycine methyl ester derivatives. The isolated compounds were tested for their cytotoxic, antimicrobial, biofilm inhibition, antiviral, and nematicidal activities. While only moderate antimicrobial effects were observed, the terphenyl quinone derivatives **3-6** and leucomelone (**10**) exhibited significant cytotoxicity against the mouse fibroblast L929 and cervix carcinoma KB-3-1 cell lines with IC_{50} values ranging from 2.4 to 26 µg/mL.

Furthermore, metabolites **4-6** showed interesting antiviral activity against hepatitis C virus (HCV).

Keywords: Secondary metabolites; Cytotoxicity; Antimicrobial activity; Antiviral activity; Terphenyl quinones; Phenylglycine methyl ester derivatives

1. Introduction

Today, the emergence of drug-resistant pathogens, drug-resistant cancer cells and the occurrence of various side effects for the currently available drugs is a problem of medical concern. In the last two decades, the problem has intensified with the emergence of multidrug resistance in many pathogens that cause human diseases. Bioactive compounds of natural origin have been the most consistent successful sources for developing novel antimicrobial drugs; hence, there is an urgent need in exploration of natural products. In this regard, the fungal kingdom provides an abundant and diverse source of bioactive metabolites as lead candidates for development of drugs and agrochemical pesticides (Bills and Gloer, 2016). Biological activities of secondary metabolites from a diverse range of microorganisms have been demonstrated in many studies. Many studies have been done on the secondary metabolites of some antagonistic fungi and many antimicrobial compounds have been identified (Helaly et al., 2017; Richter et al., 2016; Surup et al., 2017).

During a survey on *Cytospora* canker disease of walnut trees in May 2017, samples were collected from walnut trees with typical *Cytospora* canker symptoms in West Azerbaijan province of Iran. Already during the isolation procedure, it was observed that one of the strains exhibited an inhibition zone against other fungi in the agar plates. Therefore, the fungus *Cytospora* sp. strain CCTU A309 was studied for production of cytotoxic, antimicrobial, biofilm inhibition and antiviral secondary metabolites, which will be the subject of the current paper.

2. Results and discussion

2.1. Structure elucidation

Preparative RP-HPLC purification of extracts from the culture of the plant pathogenic fungus *Cytospora* sp collected in Iran led to the isolation and structure elucidation of 6 previously unreported secondary metabolites **1-6** together with 5 known ones. Compound **1**, isolated as brown oil, was assigned to the molecular formula $C_{13}H_{14}O_6$ on the basis of the HRESIMS ion cluster $[M + H]^+$ at *m/z* 267.0860 (Calcd for $C_{13}H_{15}O_6^+$: 267.0863). The ^1H

NMR spectrum showed signals for a monosubstituted benzene ring at δ_H 7.32-7.34 (5H, m, H-2', H-3', H-4', H-5', H-6'), two methine protons at δ_H 4.82 (1H, d , J = 6.7 Hz, H-2), 4.20 (1H, brd, J = 6.7 Hz, H-3) as well as two methylene groups at δ_H 2.69–2.76 (2H, m, H-5) and 2.44–2.48 (2H, m, H-6). The ^{13}C NMR spectrum showed 11 signals including those of a ketone group at δ_C 209.1 (C-4), two carboxyl carbons at δ_C 176.1 (C-1) and 176.4 (C-7), two methynes at δ_C 72.5 (C-2) and 62.7 (C-3), and two methylene carbons at δ_C 37.7 (C-5) and 28.9 (C-6) (Table 1). The presence of the monosubstituted benzene ring was evidenced by resonances depicted at δ_C 136.2 (C-1′), 131.2 (C-2′ and C-6′), 129.7 (C-3′ and C-5′), and 128.9 (C-4′). The gross structure of **1** was determined by a combination of the ^1H–^1H COSY, HSQC and HMBC spectra. The HMBC correlations depicted from H-2 (δ_H 4.82, d, J = 6.7 Hz) to carbons C-1 (δ_C 176.1), C-3 (δ_C 62.7), C-4 (δ_C 209.1) and C-1' (δ_C 136.2), from H-3 (δ_H 4.20, brd, J = 6.7 Hz) to carbons C-1 (δ_C 176.1), C-2 (δ_C 72.5), C-4 (δ_C 209.1), C-5 (δ_C 37.7) and C-2' and C-6' (δ_C131.2) as well as from H-5 (δ_H 2.69–2.76, m) to carbons C-3 (δ_C 62.7), C-4 (δ_C 209.1), C-6 (δ_C 28.9) and C-7 (δ_C176.4) established the planar structure as 2-hydroxy-3-phenyl-4-oxoheptanedioic acid. The relative stereochemistry of C-2/C-3 was addressed by a detailed *J*-based configurational analysis (Figure 2); HSQC-Hecade and *J*-HMBC NMR spectra were measured to determine the carbon-proton coupling constants. Since a ROESY correlation was observed between H-2 and H-3 together with a rather large $^3J_{H2H3}$ = 6.7 Hz coupling constant, a nearly *synperiplanar* conformation of these protons was concluded. The observed $^2J_{H3C2}$ (large) and $^3J_{H2C1'}$ (large) coupling constants indicated a *gauge* conformation between H-3/2-OH and an antiperiplanar conformation between H-2/C-1'. Taken together, a (2*R*,3*S*) was concluded. To determine the absolute stereochemistry at C-2, compound **1** was treated with both (*S*)- and (*R*)- phenylglycine methyl ester (PGME) hydrochlorides. The difference in the ^1H NMR chemical shifts ($\Delta\delta = \delta_{(S)} - \delta_{(R)}$) between (*S*) and (*R*)-PGME amides were used to assign the configuration at C-2 of α-oxy-α-monosubstituted acetic acid derivatives (Yabuuchi and Kusumi, 2000). In the ^1H NMR spectra of the amides obtained from compound **1**, H-2 gave a negative value for $\Delta\delta = \delta_{(S)} - \delta_{(R)}$ (– 0.039 ppm) indicating the *R* configuration at C-2 (Yabuuchi and Kusumi, 2000). The structure of **1** was elucidated as (2*R*,3*S*) 2-hydroxy-3-phenyl-4-oxoheptanedioic acid for which we propose the trivial name cytosporadioic acid A .

Metabolite **2** also isolated as brown oil possessed the same molecular formula as **1** as evidenced by the HRESIMS which showed a protonated molecular ion at *m/z* 267.0866 $[M+H]^+$ (calcd for $C_{13}H_{15}O_6^+$, 267.0863) despite the fact that both compounds had different retention times. Its ^1H NMR spectrum exhibited resonances for a monosubstituted benzene

ring at δ_H 7.31-7.33 (5H, m, H-1', H-2', H-3', H-4', H-5', H-6'), two methine protons at δ_H 4.62 (1H, d , J = 8.2 Hz, H-2), 4.20 (1H, d, J = 8.2 Hz, H-3) and two methylene protons at δ_H 2.74–2.79 (2H, m, H-5) and 2.45–2.49 (2H, m, H-6). The ^{13}C NMR data were similar to those of **1** with some characteristic signals at δ_C 208.5 (C-4), 175.9 (C-1) and 176.3 (C-7). The presence of two methines was evidenced by resonances observed at δ_C 74.0 (C-2) and 63.1 (C-3) (Table 1). Signals assigned to the monosubstituted benzene ring were depicted at δ_C 136.0 (C-1′), 131.2 (C-2′ and C-6′), 129.7 (C-3′ and C-5′), and 128.9 (C-4′). Detailed analysis of the ^1H and ^{13}C NMR as well as 2D-NMR data suggested that compound **2** might possess the same planar structure as metabolite **1**, with the difference of slight downfield or upfield shifts of some carbon and proton signals. A detailed *J*-based configurational analysis (Figure 2) yielded in a 2*S**,3*S** configuration, with an *anti-periplanar* conformation of H-2/H-3. To assign the absolute configuration, compound **2** was also treated with both (*S*)- and (*R*)-phenylglycine methyl ester (PGME) hydrochlorides. The difference in the ^1H NMR chemical shifts ($\Delta\delta = \delta_{(S)} - \delta_{(R)}$) between (*S*) and (*R*)-PGME amides for H-2 (+ 0.039 ppm) indicated the *S* configuration (Yabuuchi and Kusumi, 2000). The structure of **2** was thus elucidated as (2*S*,3*S*) 2-hydroxy-3-phenyl-4-oxoheptanedioic acid, the 2-epimer of metabolite **1** and trivially named cytosporadioic acid B.

The stereo chemical assignment for C–3 of **1** and **2** was confirmed by the comparison of the ^{13}C NMR shifts of the *syn* and *anti* isomers of ethyl 2-hydroxy-4-oxo-3-phenylpentanoate, which can be considered as model compounds for **1** and **2**, respectively. Ethyl 2-hydroxy-4-oxo-3-phenylpentanoate had been synthesized as a mixture of *syn*/*anti* isomers. Analogously to **1** and **2**, C-2 (δ_C 72.7 vs. 70.9) and C-3 (δ_C 62.5 vs. 61.8) are significantly more downshifted in the ^{13}C NMR spectrum of the *anti* isomer (2*R**,3*S**) compared to the *syn* derivative (2*S**,3*S**) (Pousse et al., 2010).

Compound **3**, obtained as a purple gum, exhibited in the positive ion mode HRESIMS peaks at *m/z* 407.1127 $[M+H]^+$ and 429.0947 $[M+Na]^+$ corresponding to the molecular formula $C_{23}H_{18}O_7$ (Calcd for $C_{23}H_{19}O_7^+$: 407.1125; Calcd for $C_{23}H_{18}O_7Na^+$: 429.0945). Its ^1H NMR spectrum showed in addition to two proton signals at δ_H 7.22 (s, H-6) and 7.44 (s, H-9) resonances for an AA'BB' spin system at δ_H 7.41 (d, J = 8.9 Hz, H-2' and H-6') and 6.98 (d, J = 8.9 Hz, H-3' and H-5') suggesting the presence of a *para*-disubstituted aromatic ring in the structure. The ^1H NMR spectrum further showed two olefinic methyl singlets at δ_H 1.76 (H-4") and 1.78 (H-5"), an oxygenated methylene doublet at δ_H 4.60 (J = 6.5 Hz, H-1") and a vinyl proton at δ_H 5.46 (m, H-2") assignable to a γ,γ-dimethylallyloxy moiety (Reddy et al.,

2008). The ^{13}C NMR spectrum showed 23 signals including those of 2 carbonyls at δ_C 180.3 (C-1) and 177.5 (C-4), 11 quaternary carbons, 7 methines, one methylene, and two methyl groups (Table 2). The resonances of a methylene at δ_C 65.4 (C-1"), an olefinic methine at δ_C 121.2 (C-2"), two methyl groups at δ_C 18.3 (C-4") and 25.9 (C-5") as well as the quaternary carbon at δ_C 137.9 (C-3") were assigned to the γ,γ-dimethylallyloxy moiety. Careful analysis of ^{1}H and ^{13}C NMR, ^{1}H–^{1}H COSY, HSQC and HMBC spectra showed that compound **3** was related to cycloleucomelone, a pigment previously isolated from the basidiomycete *Thelephora ganbajun* (Lin and Liu, 2001). This was further confirmed by HMBC correlations from protons at δ_H 7.22 (s, H-6) to C-8 (δ_C 146.7) and C-9a (δ_C 114.9); 7.44 (s, H-9) to C-7 (δ_C 149.2), C-5a (δ_C 152.3) and C-9b (δ_C 119.8); 7.41 (d, J = 8.9 Hz, H-2'/H-6') to C-3 (δ_C 118.8) and C-4' (δ_C 159.7); and finally from protons at δ_H 6.98 (d, J = 8.9 Hz, H-3'/H-5') to C-1' (δ_C 123.5). The location of the γ,γ-dimethylallyloxy group at C-4' was evidenced by the HMBC correlation observed between the proton signal at δ_H 4.60 (d, J = 6.5 Hz, H-1") and the carbon at δ_C 159.7 (C-4'). Consequently, metabolite **3** was elucidated as 4'-γ,γ-dimethylallyloxycycloleucomelone, for which we propose the trivial name cytosporaquinone A.

The molecular formula of compound **4** also isolated as a purple gum was established as $C_{23}H_{20}O_8$ by the positive ion mode HRESIMS which showed the ion cluster at *m/z* 425.1236 $[M + H]^+$ (Calcd for $C_{23}H_{21}O_8^+$: 425.1231). In the ^{1}H NMR spectrum, resonances attributable to a *para*-disubstituted aromatic ring at δ_H 7.47 (d, J = 8.9 Hz, H-2" and H-6") and 6.97 (d, J = 8.9 Hz, H-3" and H-5")] as well as an oxygenated tetrasubstituted benzene ring at δ_H 6.65 (s, H-2' and H-6') (Puder et al., 2005) were observed. It also showed signals for a vinyl proton at δ_H 5.49 (m, H-2"'), an oxymethylene at δ_H 4.60 (d, J = 6.6 Hz, H-1"') and two vinyl connected methyl singlets at δ_H 1.78 (H-5"') and 1.76 (H-4"') characteristic of an *O*-isoprenyl moiety as in compound **3**. The ^{13}C NMR spectrum of this metabolite showed only signals for 19 instead of 23 carbons as deduced from the mass data. In addition to resonances of the oxygenated tetrasubstituted benzene ring at δ_C 121.8 (C-1'), 111.0 (C-2' and C-6'), 145.7 (C-3' and C-5'), and 133.8 (C-4') were those of the *para*-disubstituted aromatic ring at δ_C 123.3 (C-1"), 132.8 (C-2" and C-6"), 114.7 (C-3" and C-5"), and 159.6 (C-4") (Table 3). Detailed analysis of ^{1}H–^{1}H COSY, HSQC and HMBC spectra and comparison with the literature data suggested that compound **4** was a *p*-terphenyl quinone derivative (Puder et al., 2005; Surup et al., 2016). In the HMBC spectrum, some important correlations were depicted from H-2'/H-6' to C-2 (δ_C 116.2) and C-4' (δ_C 133.8), and from H-2"/H-6" to C-5 (δ_C 115.6) and C-4" (δ_C 159.6). Furthermore, the γ,γ-dimethylallyloxy moiety was placed at C-4" as the

oxymethylene protons at δ_H 4.60 (d, J = 6.6 Hz, H-1''') correlated to C-4'' (δ_C 159.6) in the HMBC spectrum. Since 4 carbon signals were missing in the ^{13}C NMR spectrum, metabolite **4** could be a *p*-terphenyl quinone derivative in which the two hydroxyl groups of the 2,5-dihydroxybenzoquinone core are not substituted. This phenomenon has previously been observed in some related compounds and might be due to rapid interconversion of two equivalent tautomeric forms of the 2,5-dihydroxyquinone ring system (Alvi and Pu, 1999; Surup et al., 2016). Compound **4** was elucidated as 2-(3,4,5-trihydroxyphenyl)-3,6-dihydroxy-5-(4-γ,γ-dimethylallyloxyphenyl)-2,5-cyclohexadiene-1,4-dione, for which we propose the trivial name cytosporaquinone B.

The HRESIMS of compound **5** isolated as a purple gum showed ion clusters at *m/z* 409.1281 $[M+H]^+$ and 431.1103 $[M+Na]^+$ consistent with the molecular formula $C_{23}H_{20}O_7$ (Calcd for $C_{23}H_{21}O_7^+$: 409.1287; Calcd for $C_{23}H_{20}O_7Na^+$: 431.1103) indicating the lack of one oxygen atom compared to **4**. The ^1H NMR spectrum of **5** (Table 1) was closely related to that of **4** with the presence of an AA'BB' spin system at δ_H 7.47 (d, J = 8.9 Hz, H-2'' and H-6'') and 6.98 (d, J = 8.9 Hz, H-3'' and H-5'') and the γ,γ-dimethylallyloxy moiety. The main difference was that resonances of the tetrasubstituted benzene ring present in compound **4** were replaced by those of a trisubstituted aromatic ring evidenced by proton signals at 7.08 (brs , H-2'), 6.93 (brd, J = 8.2, Hz, H-6') and 6.87 (d, J = 8.2 Hz, H-5'). The ^{13}C NMR spectrum also showed only signals for 19 instead of 23 carbons as deduced from the MS data probably due to rapid interconversion of two equivalent tautomeric forms of the 2,5-dihydroxyquinone ring system as in **4**. Signals attributed to the trisubstituted aromatic ring were depicted at δ_C 122.6 (C-1'), 118.8 (C-2'), 145.1 (C-3'), 146.0 (C-4'), 115.5 (C-5'), and 123.8 (C-6') (Table 3). Careful examination of the ^1H–^1H COSY, HSQC, and HMBC spectra proved the structure of metabolite **5** to be 2-(3,4-dihydroxyphenyl)-3,6-dihydroxy-5-(4-γ,γ-dimethylallyloxyphenyl)-2,5-cyclohexadiene-1,4-dione for which we propose the trivial name cytosporaquinone C.

Metabolite **6** was obtained as a purple gum from MeOH. Its HRESIMS exhibited an ion cluster at *m/z* 393.1331 $[M + H]^+$ corresponding to the molecular formula $C_{23}H_{20}O_6$ (Calcd for $C_{23}H_{21}O_6^+$: 393.1333) and indicating the lack of one oxygen atom as compared to **5**. The ^1H NMR spectrum showed in addition to signals attributed to the γ,γ-dimethylallyloxy moiety two sets of *para*-substituted phenyl ring system [δ_H 6.88 (d, J = 8.7 Hz, H-3' and H-5'), 7.42 (d, J = 8.7 Hz; H-2' and H-6'); and 6.96 (d, J = 8.8 Hz, H-3'' and H-5''), 7.50 (d, J = 8.8 Hz, H-2'' and H-6'')]. In the ^{13}C NMR spectrum, signals depicted at at δ_C 121.7 (C-1'), 122.8 (C-1''), 131.9 (C-2' and C-6'), 131.7 (C-2'' and C-6''), 114.3 (C-3' and C-5'), 113.7 (C-

3" and C-5"), 156.9 (C-4'), and 158.5 (C-4") confirmed the presence of the *para*-substituted phenyl ring system (Table 3). HMBC correlations observed from protons at δ_H 7.42 (d, J = 8.7 Hz, H-2'/H-6') to C-2 (δ_C 114.7) and C-4' (δ_C 156.9); 7.50 (d, J = 8.8 Hz, H-2"/H-6") to C-5 (δ_C 114.3) and C-4" (δ_C 158.5); and finally from protons at δ_H 4.60 (d, J = 6.5 Hz, H-1"') to C-4" (δ_C 158.5) established the structure of **6** as 2-(4-hydroxyphenyl)-3,6-dihydroxy-5-(4-γ,γ-dimethylallyloxyphenyl)-2,5-cyclohexadiene-1,4-dione, for which we propse the trivial name cytosporaquinone D.

Known compounds were identified as 3-(2-carboxy-2,5-dihydro-4-hydroxy-5-oxo-3-phenyl-2-furyl)propionic acid (**7**) (Küppers et al., 2017), 3-(2,5-dihydro-4-hydroxy-5-oxo-3-phenyl-2-furyl)propionic acid (**8**) (Lu et al., 2011), 3,5-dimethyl-8-methoxy-3,4-dihydroisocoumarin (**9**) (Kamisuki et al., 2007; Kokubun et al., 2003), leucomelone (**10**) (Zheng et al., 2006), and atromentin (**11**) (Hu and Liu, 2003; Zheng et al., 2006). Compounds **7** and **8** are related butenolides, reported to be produced by several ascomycetes, including *Talaromyces rugulosus* (Küppers et al., 2017), *Acremonium* sp. (Ghisalberti et al., 2004) and even already known from another *Cytospora* sp (Lu et al., 2011). Due to the structural similarity between the two heptanedioic acid derivatives **1** and **2** and these butanolides, we proposed a plausible biogenetic pathways for the formation of the new metabolites. Decarboxylation of compound **7** could yield metabolite **8** which after the reduction of the C_2–C_3 double bond yields two stereomers **12** and **13**. Hydrolysis of **12** and **13** could afford the heptanedioic acid derivative **14** and **15**, which upon selective oxidation of the hydroxyl group at C-4 finally yield compounds **1** and **2** (Fig. 3). Compounds **3**-**6** are terphenyls, a class of fungal pigments reported to exhibit various biological activities. They are potent immunosuppressants and exert neuroprotective, antithrombotic, anticoagulant, specific 5-lipoxygenase inhibitory, and cytotoxic activities (Liu, 2006). Recently, their antimicrobial potential was shown (Li et al., 2016; Surup et al., 2016). Regarding the biosynthesis, it has been established by feeding ^{13}C- and ^{14}C-labeled precursors to the growing cultures that *p*-terphenyls arise by initial condensation between two molecules of either phenylpyruvic acid or phenylalanine (Liu, 2006).

2.2. Antimicrobial Activity and Cytotoxicity Assay

The isolated compounds were evaluated for their antimicrobial activity. Compounds **1** and **11** showed rather weak antifungal activity against *Mucor hiemalis* DSM 2656 and *Rhodoturula glutinis* DSM 10134, respectively with MIC value of 66.66 µg/mL while compounds **2** and **7**-**9** showed exhibited weak antifungal activity against *Mucor hiemalis* DSM 2656 and *Rhodoturula glutinis* DSM 10134 with MIC value of 66.66 µg/mL.

Compounds **3-6**, **10** showed moderate to weak antimicrobial activity against all the tested fungi, Gram-positive and Gram-negative bacteria with MIC values from 16.66 to 66.66 µg/mL (Table 4). The results obtained are in accordance with literature since Surup et al. (2016) also reported antimicrobial and cytotoxic effects of terphenyl derivatives.

Significant cytotoxicity was observed for terphenylquinone derivatives **3-6** and **10** against the mouse fibroblast cell line L929 and cervix carcinoma cell line KB-3-1, with IC_{50} values ranging from 2.4 to 26 µg/ml (Table 5) while in the case of compounds **1**, **2** and **7-9**, no significant effect was observed.

2.3. Anti-biofilm assay

Compounds **1-11** were tested for their ability to inhibit formation of biofilms of *Staphylococcus aureus* and *Pseudomonas aeruginosa*. All tested compounds were inactive against *P. aeruginosa* biofilm formation, while they showed significant activity against *S. aureus* (Table 6). Compounds **6** and **7** showed strong biofilm inhibition activity. They showed an inhibition of biofilm formation of 86.92% and 85.9% at 256 µg/ml, respectively, while MIC was not obtained for compound **7**. In fact, compound 7 was not toxic against planktonic cells at this concentration, where 86.92% of the biofilm was prevented and still 40.60% of the biofilm was prevented at 4 µg/ml. Even compounds **1**, **2**, **8** and **9** were not toxic against planktonic cells at 256 µg/ml but they showed significant inhibition of biofilm formation at lower concentrations. Of the tested compounds, only compound **6** was able to disperse pre-formed biofilm, (it dispersed 68.05% of pre-formed biofilm at the concentration of 256 µg/ml). Biofilm formation is an important factor associated with drug resistance. Biofilms play a protective role against unfavorable conditions, and eradication of biofilm infections is difficult. To overcome these difficulties together with increasing antibiotic resistances the need for new and useful pharmaceutical compounds, is felt more than ever for the treatment of various infection (Austin et al., 1999). There is also an urgent need for compounds with biofilms dispersing properties even if compounds with this feature are rare (Estrela and Abraham, 2016). The only compound class that we have so far encountered in our screening for biofilm dispersers were the microporenic acids (Chepkirui et al., 2018), which were, however, more active against *Candida albicans* than against pathogenic bacteria.

2.4. Inhibitory effects on HCV Infectivity

The results obtained for the antiviral activity against HCV in human liver cells (Figs. 4 and 5) showed that only the terphenyl quinone derivatives **4**, **5** and **6** significantly inhibited HCV infectivity in a dose-dependent manner. Importantly, the active compounds showed no cytotoxicity on the liver cells. While the terphenyls **3** and **11** were found devoid of antiviral

activity, compound **10** already showed weak cytotoxicity at the initial concentration of 40 µM and was not tested further. The data available do not allow to establish structure-activity relationships, but it might be worthwhile to test additional compounds of this type, which are widely available for other fungi, against HCV.

2.5. Nematicidal activity

In the case of compounds **1**, **2**, **7**and **8**, significant mortality was not observed, while metabolites **4**-**6** and **11** showed some mortality at the highest concentration (100 µg/mL), but the IC_{50} values were not obtained.

3. Conclusion

Eleven metabolites including two previously unreported heptanedioic acid derivatives namely (2*R*,3*R*) 2-hydroxy-3-phenyl-4-oxoheptanedioic acid (**1**) and (2*S*,3*S*) 2-hydroxy-3-phenyl-4-oxoheptanedioic acid (**2**), and four previously undescribed prenylated *p*-terphenyl quinones **3**-**6** were isolated from a culture of the plant pathogenic fungus *Cytospora* sp that was characterised to the genus level by means of morphological studies and molecular phylogenetic methods. The absolute configurations of compounds **1** and **2** were deduced from comparison of the ^{1}H NMR difference of their (*S*)- and (*R*)-phenylglycine methyl ester derivatives. The new *p*-terphenyl quinone derivatives exhibited significant cytotoxicity against the mouse fibroblast L929 and cervix carcinoma KB-3-1 cell lines with IC_{50} values ranging from 2.4 to 26 µg/mL and showed interesting antiviral activity against hepatitis-C-virus.

4. Experimental section

4.1. General experimental procedures

1D and 2D NMR spectra were recorded on a Bruker 500 MHz Avance III spectrometer with a BBFO (plus) SmartProbe (^{1}H 500 MHz, ^{13}C 125 MHz) and a Bruker 700 MHz Avance III spectrometer with a 5 mmTCI cryoprobe (^{1}H 700 MHz, ^{13}C 175 MHz). Chemical shifts are given in parts per million (ppm), and coupling constants in hertz (Hz). Spectra were measured in acetone-d_6 and methanol-d_4 while chemical shifts were referenced to the solvent signals. Optical rotations were measured with a Perkin Elmer 241 MC polarimeter (using the sodium D line and a quartz cuvette with a 10 cm path length and 0.5 mL volume). UV spectra were recorded with a Shimadzu UV–vis spectrophotometer UV-2450. HPLC-DAD-MS analysis was performed using an amaZon speed ETD ion trap mass spectrometer (Bruker Daltonics) in positive and negative ionization modes. The mass spectrometer was coupled to an DIONEX UltiMate 3000 Diode Array Detector [column 2.1

× 50 mm, 1.7 µm, C18 Acquity UPLC BEH (Waters), solvent A: H_2O + 0.1% formic acid; solvent B: acetonitrile (ACN) + 0.1% formic acid, gradient: 5% B for 0.5 min, increasing to 100% B in 20 min, maintaining isocratic conditions at 100% B for 10 min, flow = 0.6 mL/min, UV−vis detection 190−600 nm]. HRESIMS mass spectra were obtained with a maXis ESI TOF mass spectrometer (Bruker Daltonics) [scan range m/z 100−2500, rate 2 Hz, capillary voltage 4500 V, dry temperature 200 °C], coupled to an Agilent 1200 series HPLC-UV system [column 2.1 × 50 mm, 1.7 µm, C_{18} Acquity UPLC BEH (Waters), solvent A: H_2O + 0.1% formic acid; solvent B: ACN + 0.1% formic acid, gradient: 5% B for 0.5 min, increasing to 100% B in 19.5 min, maintaining 100% B for 5 min, R_F = 0.6 $mLmin^{-1}$, UV−vis detection 200−600 nm]. The molecular formulas were calculated including the isotopic pattern (Smart Formula algorithm). Preparative HPLC purification was performed at room temperature on an Agilent 1100 series preparative HPLC system [ChemStation software (Rev. B.04.03 SP1); binary pump system; column: Kinetex 5u RP C18, dimensions 250 × mm; mobile phase: ACN + 0.05% trifluoroacetic acid (TFA) and water + 0.05% TFA; flow rate 20 mL/min; diode-array UV detector; 226 fraction collector].

4.2. Fungal material and morphological analysis

For the isolation of *Cytospora* sp. (CCTU A309), infected *Juglans* branches were surface-sterilized for 2-3 minutes in 70% sodium hypochlorite (NaClO), then small pieces were cut from the margins of infected tissues and surface-sterilized for another 45-60 seconds in 70% ethanol and rinsed with sterile distilled water for three times. After drying on sterile filter paper, the samples were transferred on Potato Dextrose Agar (PDA) plates supplemented with 100 mg/L streptomycin sulphate and 100 mg/L ampicillin. Purification of the culture was conducted by using the hyphal tip technique. Cultures were preserved on MEA (malt extract agar) in 2 mL microtube slants at 4°C in the University of Tabriz Culture Collection (CCTU A309). Cultural characteristics of *Cytospora* isolates including colony characters and pigment production were recorded on PDA, MEA and OA in darkness at 25 °C after 7 and 14 days. Radial growth of colony was measured after 7 days.

4.3. Molecular analysis, sequencing and phylogenetic analysis

Genomic DNA was extracted using the EZ-10 Spin Column Genomic DNA Miniprep kit (Bio Basic Canada Inc., Markham, Ontario, Canada) following the manufacturer's protocol. Molecular analysis was carried out using sequence data of internal transcribed spacer (ITS) regions (using ITS1F/ITS4 primer) (White et al., 1990) and translation elongation factor 1-a (TEF1-a) fragments (using primers EF1-728F/EF1-986R) (Carbone and Kohn, 1999). Sequence files were edited using SeqMan software in the Lasergene package

(DNASTAR Inc., Madison, WI, USA) and consensus sequence was compared with sequences in the GenBank using the Basic local alignment search tool (BLAST). Sequences were deposited in GenBank with the accession numbers MH819654 and MH822660 for ITS aNd TEF, respectively. Bayesian analyses were accomplished according to previously published procedure (Narmani et al., 2018).

4.4. Fermentation and Extraction

Six 7 mm agar disks of a well-grown agar culture of *Cytospora* (7 days old) were used for inoculation of a 500 mL Erlenmeyer flask containing 200 mL of Q6 1/2 medium consisting of 0.25% glucose, 1% glycerin, 0.5% cotton seed flour, pH 7.2 and incubated at 23 °C. The culture medium was homogenized using a Heidolph Silent Crusher when the glucose content of the medium reached 50 mg. About 2 ml of the homogenized culture was used to inoculate 30 other flasks containing the same medium composition. The flasks were incubated at 23 °C under constant shaking at 140 rpm on a rotary shaker. 5 days after the sugar was used up, the fungal mycelium was separated by filtration and the supernatant was treated with 2% adsorber resin Amberlite XAD-16N over 2 h at room temperature. Then, XAD was extracted with acetone and the solution obtained was evaporated to yield an aqueous phase, which was further extracted with ethyl acetate (3x500 mL). The ethyl acetate fraction was dried over anhydrous Na_2SO_4, filtered, and concentrated under vacuum to yield 750 mg of extract. The wet mycelium was extracted three times with acetone, then with methanol in an ultrasonic bath at 40°C for 30 min. The resulting solution was evaporated to yield an aqueous phase, which was also extracted with ethyl acetate (3×500 mL). After drying over anhydrous Na_2SO_4, the ethyl acetate fraction was concentrated under vacuum to yield 3114.8 mg of crude mycelial extract.

A 500 mL Erlenmeyer flask containing rice medium consisting of 35 g brown rice, 0.15 g peptone, 0.05 g corn syrup, 50 mL water, pH 7, was also inoculated with five 7 mm agar disks of a well-grown agar culture of *Cytospora* (7 days old). The fermentation was carried out at 23 °C under static conditions for 30 days. The culture medium was extracted with EtOAc to give 88 mg of crude extract.

*4.5. Isolation of compounds **1-11***

Fractionation of the supernatant crude extract (400 mg) was achieved by preparative HPLC (4 runs using a linear gradient of solvent B from 10% to 30% solvent B in 45 min, 30 to 100% B in 5 min followed by isocratic conditions for 10 min at a flow rate of 20 ml/min. Fractions were collected and combined according to UV absorption at 220, 280, and 350 nm and concurrent HPLC-MS analyses. The separation yielded compounds **1** (15.2 mg, Rt =

15.03 min, **2** (78 mg, Rt = 15.93 min), **7** (21 mg, Rt = 21.83 min), **8** (4.15 mg, Rt = 35.50 min), and **9** (3.12 mg, Rt = 40.18 min). The mycelial extract (400 mg) was purified by preparative HPLC (4 runs) using a linear gradient of solvent B from 35% to 55% solvent B in 45 min, 55 to 100% B in 5 min, and isocratic condition for 10 min at a flow rate of 20 ml/min. Fractions were collected and combined according to UV absorptions at 220, 280, and 350 nm. The separation yielded compounds **4** (28.24 mg, Rt = 25.90 min), **5** (6.94 mg, Rt = 31.94 min), **3** (3.67 mg, Rt = 36.46 min), and **6** (8.68 mg, Rt = 37.42 min). Crude extract from the culture on rice medium (88 mg) was fractionated using the gradient from 14% to 27% solvent B in 45 min, 45 to 100% B in 5 min, then 100% B for 10 min at a flow rate of 20 mL/min. Fractions were collected and combined according to UV absorptions at 220, 280, and 350 nm. The separation yielded compounds **10** (2.28 mg, Rt = 26.04 min) and **11** (3.43 mg, Rt = 38.45 min) along with further metabolites which were not identified conclusively because of their low amounts.

*4.5.1. Cytosporadioic acid A (**1**)*

Brown oil; $[\alpha]^{25}_{D}$ + 132.1 (*c* 0.0083, MeOH); UV (MeOH, *c* 0.25 mg/mL) λ_{max} (log ε) 279 (2.78), 218 (3.67) nm; ^{1}H NMR (Acetone-d_6, 500 MHz) and ^{13}C NMR (Acetone-d_6, 125 MHz) data, see Table 1; HRESIMS *m/z* 267.0860 $[M + H]^+$ (Calcd for $C_{13}H_{15}O_6^+$: 267.0863).

*4.5.2. Cytosporadioic acid B (**2**)*

Brown oil; $[\alpha]^{25}_{D}$ – 87.4 (c 0.0083, MeOH); UV (MeOH, *c* 0.25 mg/mL) λ_{max} (log ε) 285 (2.92), 219 (3.66) nm; ^{1}H NMR (Acetone-d_6, 500 MHz) and ^{13}C NMR (Acetone-d_6, 125 MHz) data, see Table 1; HRESIMS *m/z* 267.0866 $[M + H]^+$ (Calcd for $C_{13}H_{15}O_6^+$: 267.0863).

*4.5.3. Cytosporaquinone A (**3**)*

Purple gum; UV (MeOH, *c* 0.2 mg/mL) λ_{max} (log ε) 297 (4.24), 261 (4.34), 203 (4.55) nm; ^{1}H NMR (Acetone-d_6, 700 MHz) and ^{13}C NMR (Acetone-d_6, 175 MHz) data, see Table 2; HRESIMS *m/z* 407.1127 $[M+H]^+$ (Calcd for $C_{23}H_{19}O_7^+$: 407.1125), 429.0947 $[M+Na]^+$ (Calcd for $C_{23}H_{18}O_7Na^+$: 429.0945).

*4.5.4. Cytosporaquinone B (**4**)*

Purple gum; UV (MeOH, *c* 0.2 mg/mL) λ_{max} (log ε) 273 (4.65), 206 (4.76) nm; ^{1}H NMR (Acetone-d_6, 500 MHz) and ^{13}C NMR (Acetone-d_6, 125 MHz) data, see Table 3; HRESIMS *m/z* 425.1236 $[M + H]^+$ (Calcd for $C_{23}H_{21}O_8^+$: 425.1231).

4.5.5. *Cytosporaquinone C (**5**)*

Purple gum; UV (MeOH, *c* 0.2 mg/mL) λ_{max} (log ε) 358 (3.54), 269 (4.48), 204 (4.64) nm; ^{1}H NMR (Acetone-d_6, 500 MHz) and ^{13}C NMR (Acetone-d_6, 125 MHz) data, see Table

3; HRESIMS *m/z* 409.1281 $[M+H]^+$ (Calcd for $C_{23}H_{21}O_7^+$: 409.1287), 431.1103 $[M+Na]^+$ (Calcd for $C_{23}H_{20}O_7Na^+$: 431.1103).

*4.5.6. Cytosporaquinone D (**6**)*

Purple gum; UV (MeOH, *c* 0.2 mg/mL) λ_{max} (log ε) 360 (3.47), 270 (4.41), 203 (4.50) nm; ^{1}H NMR (Acetone-d_6, 500 MHz) and ^{13}C NMR (Acetone-d_6, 125 MHz) data, see Table 3; HRESIMS *m/z* 393.1331 $[M + H]^+$ (Calcd for $C_{23}H_{21}O_6^+$: 393.1333).

*4.6. Preparation of the (S) and (R)-phenylglycine methyl ester (PGME) amides of **1** and **2***

Two portions of compound **1** (3 mg) were dissolved in dry pyridine (3 mg) and 1-ethyl-3-(3-dimethylaminopropyl)carbodiimide (5 mg), 4-dimethylaminopyridine (catalytic amounts), and (*S*) or (*R*)- phenylglycine methyl ester hydrochloride (6 mg) were added. After stirring at room temperature for 16 h, the solvent was removed under reduced pressure. Each residue was dissolved in 500 µL of methanol and purified by preparative HPLC [ChemStation software (Rev. B.04.03 SP1); binary pump system; column: Kinetex 5u RP C18, dimensions 250 × 21.20 mm; mobile phase: ACN + 0.05% trifluoroacetic acid (TFA) and water + 0.05% TFA; flow rate 20 mL/min; diode-array UV detector; 226 fraction collector. The gradient from 35 to 50 % solvent B in 45 min was used] to yield (*R*)-PGME (1.19 mg, Rt = 30.65 min) of and (*S*)-PGME (1.10 mg, Rt = 30.65 min) of compound **1**, respectively. Compound **2** was treated in the same manner to give its (*R*)-PGME (1.26 mg, Rt = 26.64 min) and (*S*)-PGME (1.15 mg, Rt = 1.15 min) derivatives, respectively.

4.7. Biological activities

4.7.1. Antimicrobial activity and cytotoxicity assay

Minimum inhibitory concentrations (MICs) in µg/mL of the isolated compounds were determined with a serial dilution assay against various bacteria and fungi (Table 4) according to a previously reported procedure (Richter et al., 2016). The *in vitro* cytotoxicity was determined against the mouse fibroblast cell line L929 and cervix carcinoma cell line KB-3-1 (Sandargo et al., 2017).

4.7.2. Staphylococcus aureus and Pseudomonas aeruginosa biofilm assays

The inhibition of biofilm formation against *Staphylococcus aureus* DSM 1104 and *Pseudomonas aeruginosa* PA14 was performed in 96-well tissue microtiter plates (TPP, Trasadingen, Switzerland) following the protocol of Yuyama et al. (2017). The compounds were tested in concentrations of up to 256 µg/mL. MeOH and coprinuslactone were used as negative and positive control, respectively (De Carvalho et al. 2016).

4.7.3. Inhibitory effects on HCV infectivity

Compounds **1-11** were tested for their antiviral activity. Huh-7.5 cells were inoculated with RLuc Jc1 reporter viruses in the presence of different compounds. Monolayers were washed three times with PBS 4 hours later and overlaid with fresh medium without inhibitors. Infected cells were lysed 3 days later, and reporter virus infection was determined by renilla luciferase activity. The cell viability was measured by determination of firefly luciferase. Huh-7.5 cells stably expressing Firefly luciferase (Huh-7.5 Fluc) were cultured in Dulbecco's modified minimum essential medium (DMEM, Life Technologies Manchester UK) (containing 2 mM/L glutamine, 1 × minimum essential medium nonessential amino acids (MEM NEAA, Life Technologies), 100 μg/mL streptomycin, 100 IU/mL penicillin (Life Technologies), 5 μg/mL blasticidin and 10% fetal bovine serum). Cells were incubated at 37 °C with 5% CO_2 supply. Infected cells were lysed and then frozen at −80 °C for 1 hour following measurements of Renilla and Firefly luciferase activities on a Berthold Technologies Centro XS3 Microplate Luminometer as indicators of viral genome replication and cell viability, respectively (Von Hahn et al., 2011; Mulwa et al., 2018).

4.7.4. Nematicidal activity

In the case of compounds **1**, **2**, **4-8** and **11** which were in large amount, nematicidal activities were assessed using *Caenorhabditis elegans* in a microtiter plate assay as described by Rupcic et al. (2018). The assay was performed in four concentrations (100, 50, 25 and 12.5 μg/mL). Ivermectin was used as positive control at the same concentration ranges as the test compounds and MeOH was used as negative control. Percentage of mortality was calculated, then the results were expressed as a LD_{90} and LD_{50}.

Acknowledgements

The Ministry of Science, Research and Technology (MSRT) of Iran, the Iranian Mycological Society and the Alexander von Humboldt Foundation are gratefully acknowledged for their financial support. We are grateful to Christel Kakoschke, Sabrina Karwehl, Cäcilia Bergmann, Vanessa Stiller and Wera Collisi for recording spectra and expert technical assistance, respectively.

Appendix A. Supplementary data

Supplementary data related to this article can be found at……

References

Alvi, K.A., Pu, H., 1999. Asterriquinones produced by *Aspergillus candidus* inhibit binding of the Grb-2 adapter to phosphorylated EGF receptor tyrosine kinase. J. Antibiot. 52, 215–223.

Austin, D.J., Kristinsson, K.G., Anderson R.M., 1999. The relationship between the volume of antimicrobial consumption in human communities and the frequency of resistance. Proc. Natl. Acad. Sci. USA 96, 1152–1156.

Bills, G.F., Gloer, J.B., 2016. Biologically active secondary metabolites from the fungi. Microbiol. Spectr. 4 (DOI: 10:1128/microbiolspec.FUNK-0009-2016).

Carbone, I., Kohn, L.M., 1999. A method for designing primer sets for speciation studies in filamentous ascomycetes. Mycologia 91, 553–556.

Chepkirui, C., Yuyama, K., Wanga, L., Decock, C., Matasyoh, J., Abraham, W.R., Stadler, M., 2018. Microporenic acids A-G, biofilm inhibitors and antimicrobial agents from the basidiomycete *Microporus* sp. J. Nat. Prod. 81, 778-784.

De Carvalho, M.P., Gulotta, G., do Amaral, M.W., Lünsdorf, H., Sasse, F., Abraham W.R., 2016. Coprinuslactone protects the edible mushroom *Coprinus comatus* against biofilm infections by blocking both quorum-sensing and MurA. Environ. Microbiol. 18, 4254–4264.

Estrela, A.B., Abraham, W.R., 2016. Fungal metabolites for the control of biofilm infections. Agriculture 6, 37–62.

Ghisalberti, E.L., Hargreaves, J.R., McConville, E., 2004. Butenolides from a cultured microfungus, *Acremonium* sp. Nat. Prod. Res. 18, 105–109.

Helaly, S.E., Kuephadungphan, W., Phongpaichit, S., Luangsa-ard, J.J., Rukachaisirikul ,V., Stadler, M., 2017. Five unprecedented secondary metabolites from the spider parasitic fungus *Akanthomyces novoguineensis*. Molecules 22, 991, https://doi.org/10.3390/molecules22060991.

Hu, L., Liu, J.K., 2003. *p*-Terphenyls from the basidiomycete *Thelephora aurantiotincta*. Z. Naturforsch 58c, 452–454.

Kamisuki, S., Ishimaru, C., Onoda, K., Kuriyama, I., Ida, N., Sugawara, F., Yoshida, H., Mizushina, Y., 2007. Nodulisporol and Nodulisporone, novel specific inhibitors of human DNA polymerase k from a fungus, *Nodulisporium sp*. Bioorg. Med. Chem. 15, 3109–3114.

Keller, N.P., Turner, G., Bennett, J.W., 2005. Fungal secondary metabolism - from biochemistry to genomics. Nat. Rev. Microbiol. 3, 937–947.

Kokubun, T., Veitch, N.C., Bridge, P.D., Simmonds, M.S.J., 2003. Dihydroisocoumarins and a tetralone from *Cytospora eucalypticola*. Phytochemistry 62, 779–782.

Küppers, L., Ebrahim, W., El-Neketi, M., Özkaya, F.C., Mándi, A. , Kurtán, T., Orfali, R.S., Müller, W.E.G., Hartmann, R., Lin, W., Song, W., Liu, Z., Proksch, P., 2017. Lactones from the sponge-derived fungus *Talaromyces rugulosus*. Mar. Drugs, 15, 359, doi:10.3390/md15110359.

Li, W., Gao, W., Zhang, M., Li, Y.L., Li, L., Li, X.B., Chang, W.Q., Zhao, Z.T., Lou, H.X., 2016. p-Terphenyl derivatives from the endolichenic fungus *Floricola striata*. J. Nat. Prod. 79, 2188–2194.

Lin, H., Liu, J.-K., 2001. Two novel phenylacetoxylated *p*-terphenyls from *Thelephora ganbajun* Zang. Z. Naturforsch. 56c, 983–987.

Liu, J.K., 2006. Natural terphenyls: Development since 1977. Chem. Rev. 106, 2209–2223.

Lu, S., Draeger, S., Schulz, B., Krohn, K., Yi, Y., Li, L., Zhang, W., 2011. Bioactive aromatic derivatives from endophytic fungus, *Cytospora* sp. Nat. Prod. Commun. 6, 661–666.

Mulwa, L.S., Jansen, R., Praditya, D.F., Mohr, K.I., Wink, J., Steinmann, E., Stadler, M., 2018. Six heterocyclic metabolites from the Myxobacterium *Labilithrix luteola*. Molecules 23, 542, doi:10.3390/molecules23030542.

Narmani, A., Pichai, S., Palani, P., Arzanlou, M., Surup, F., Stadler, M., 2018. *Daldinia sacchari* (Hypoxylaceae) from India produces the new cytochalasins Saccalasins A and B and belongs to the *D. eschscholtzii* species complex. Mycol. Prog. https://doi.org/10.1007/s11557-018-1413-6.

Pousse, G., Le Cavelier, F., Humphreys, L., Rouden, J., Blanchet, J., 2010. Brønsted acid catalyzed aldol reaction. Org. Lett. 12, 3582–3585.

Puder, C., Wagner, K., Vettermann, R., Hauptmann, R., Potterat, O., 2005. Terphenylquinone inhibitors of the Src protein tyrosine kinase from *Stilbella* sp. J. Nat. Prod. 68, 323–326.

Reddy, R.V.N., Reddy, N.P., Khalivulla, S.I., Reddy, M.V.B., Gunasekar, D., Blond, A., Bodo, B., 2008. *O*-Prenylated flavonoids from *Dalbergia sissoo*. Phytochem. Lett. 1, 23–26.

Richter, C., Helaly, S.E., Thongbai, B., Hyde, K.D., Stadler, M., 2016. Pyristriatins A and B: Pyridino-cyathane antibiotics from the basidiomycete *Cyathus* cf. *striatus*. J. Nat. Prod. 79, 1684–1688.

Rupcic. Z., Chepkirui, C., Hernández-Restrepo, M., Crous, P.W, Luangsa-Ard, J.J., Stadler, M., 2018. New nematicidal and antimicrobial secondary metabolites from a new species in the new genus, *Pseudobambusicola thailandica*. MycoKeys 33, 1–23.

Sandargo, B., Thongbai, B., Stadler, M., Surup, F., 2017. Cysteine-derived pleurotin congeners from the nematode-trapping basidiomycete *Hohenbuehelia grisea*. J. Nat. Prod. 81, 286–291.

Surup, F., Wiebach, V., Kuhnert, E., Stadler, M., 2016. Truncaquinones A and B, asterriquinones from *Annulohypoxylon truncatum*. Tetrahedron Lett. 57, 2183–2185.

Surup, F., Kuhnert, E., Böhm, A., Wiebach, V., Solga, D., Engler, H., Pendzialek, T., Berkessel, A., Stadler, M., Kalesse, M., 2017. The rickiols, 20-, 22-, and 24-membered macrolides from the ascomycete *Hypoxylon rickii*. Chem. Eur. J. 24, 2200–2213. https://doi.org/10.1002/chem.201704928

Von Hahn, C.S., Colpitts, T., Schang, C.C., Friesland, L.M., Steinmann, M., Manns, J., Ott, M.P., Wedemeyer, M., Meuleman, H., Pietschmann, T., et al., 2011. The green tea polyphenol, epigallocatechin-3-gallate, inhibits hepatitis C virus entry. Hepatology 54, 1947–1955.

White, T.J., Bruns, T., Lee, S.J., Taylor, J.L., 1990. Amplification and direct sequencing of fungal ribosomal RNA genes for phylogenetics. PCR protocols: a guide to methods and applications. (pp. 315–322). New York, NY, USA: Academic Press, Inc.

Yabuuchi, T., Kusumi, T., 2000. Phenylglycine methyl ester, a useful tool for absolute configuration determination of various chiral carboxylic acids. J. Org. Chem. 65, 397−404.

Yuyama, K.T., Neves, T.S.P.C., Memória, M..T, Tartuci, I.T., Abraham, W., 2017. Aurantiogliocladin inhibits biofilm formation at subtoxic concentrations. AIMS Microbiol, 3, 50–60.

Zheng, C.J., Sohn, M.J., Kim, W.G., 2006. Atromentin and Leucomelone, the first inhibitors specific to enoyl-ACP reductase (FabK) of *Streptococcus pneumoniae*. J. Antibiotics 59, 808–812.

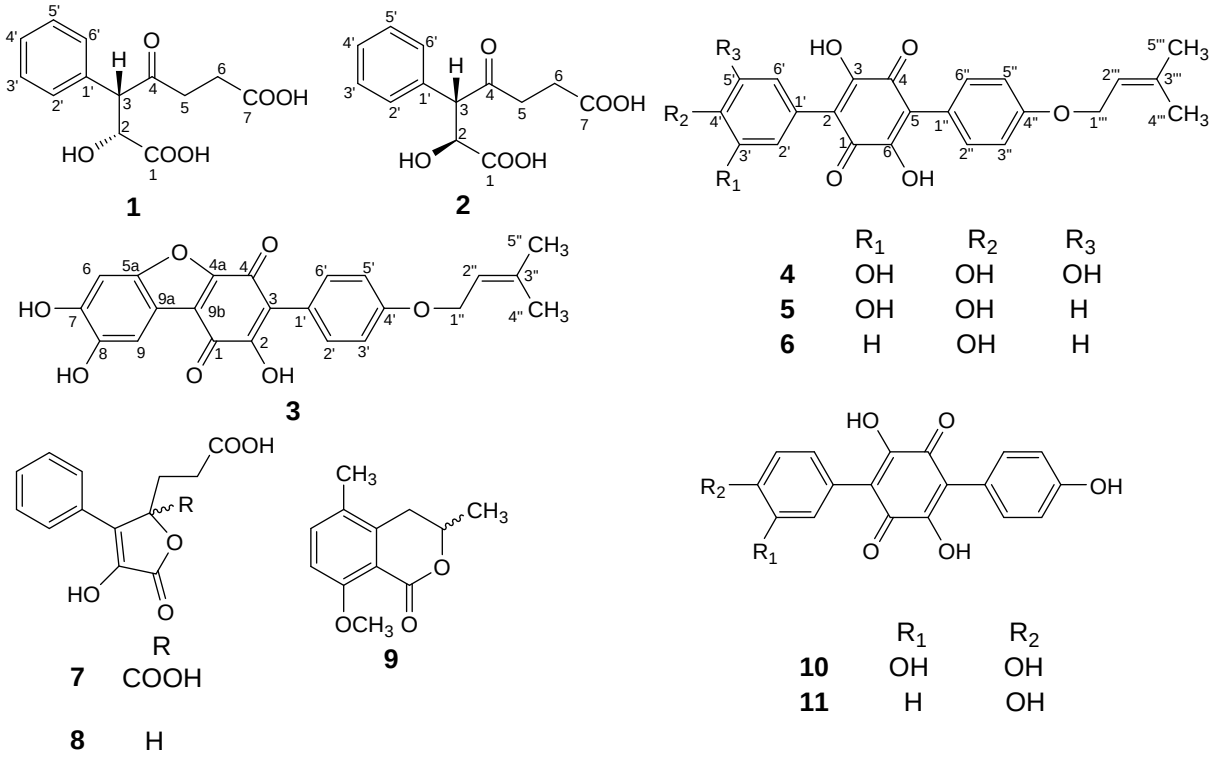

Fig. 1. Structures of compounds **1-11** isolated from *Cytospora* sp. (CCTU A309).

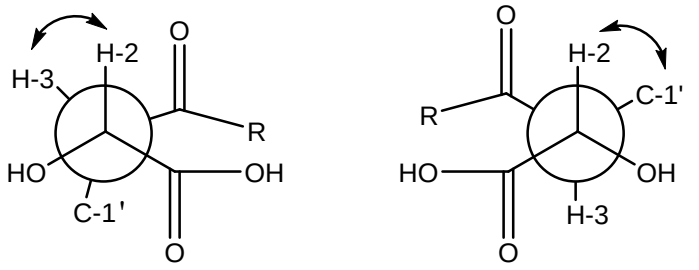

^{3}J(H-2,H-3) = 6.7 Hz
^{2}J(H-3,C-2) = 4.5 Hz
^{3}J(H-2,C-1') = 4.4 Hz

^{3}J(H-2,H-3) = 8.2 Hz
^{2}J(H-3,C-2) = 5.6 Hz
^{3}J(H-2,C-1') = 2.2 Hz
^{3}J(H-2,C-4) = 4.0 Hz

Fig. 2. *J*-based analysis of **1** (left) and **2** (right); arrows indicate ROESY correlations.

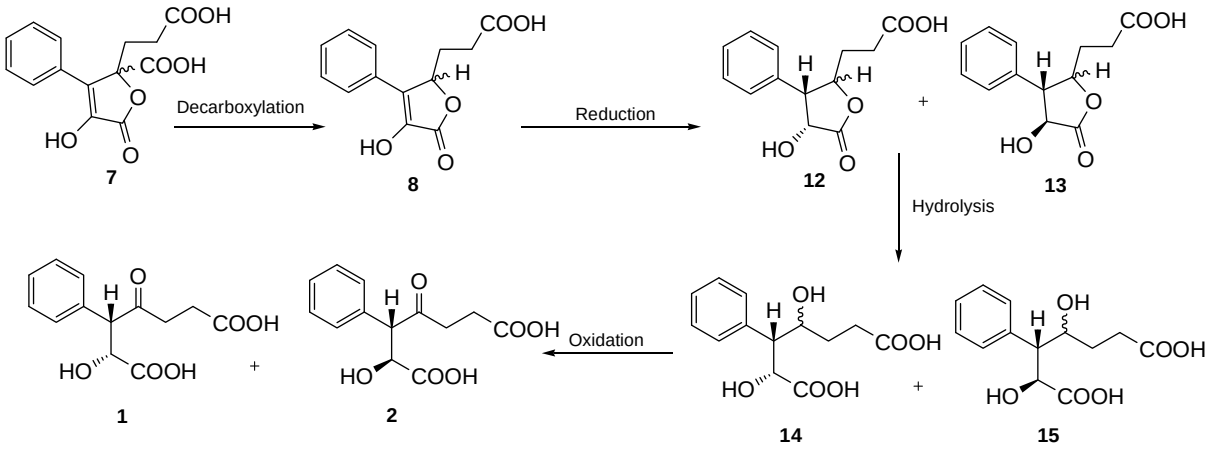

Fig. 3. Proposed biogenetic pathway for the formation of compounds **1** and **2** from butenolides **7** and **8**.

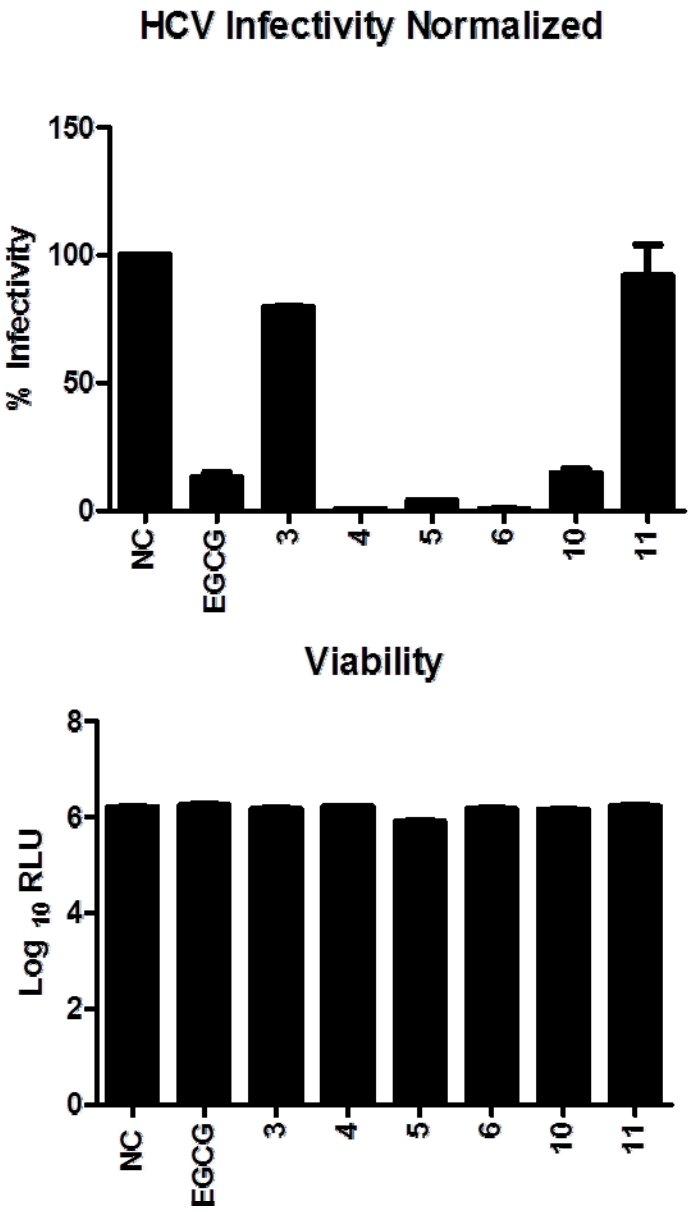

Fig. 4. Antiviral activity of the metabolites **3**-**6** and **10**-**11** from *Cytospora* sp. against Hepatitis C virus (HCV). Above: inhibition of infectivity at a starting concentration of 40 M; (lack of) cytotoxic effects at the same concentration.

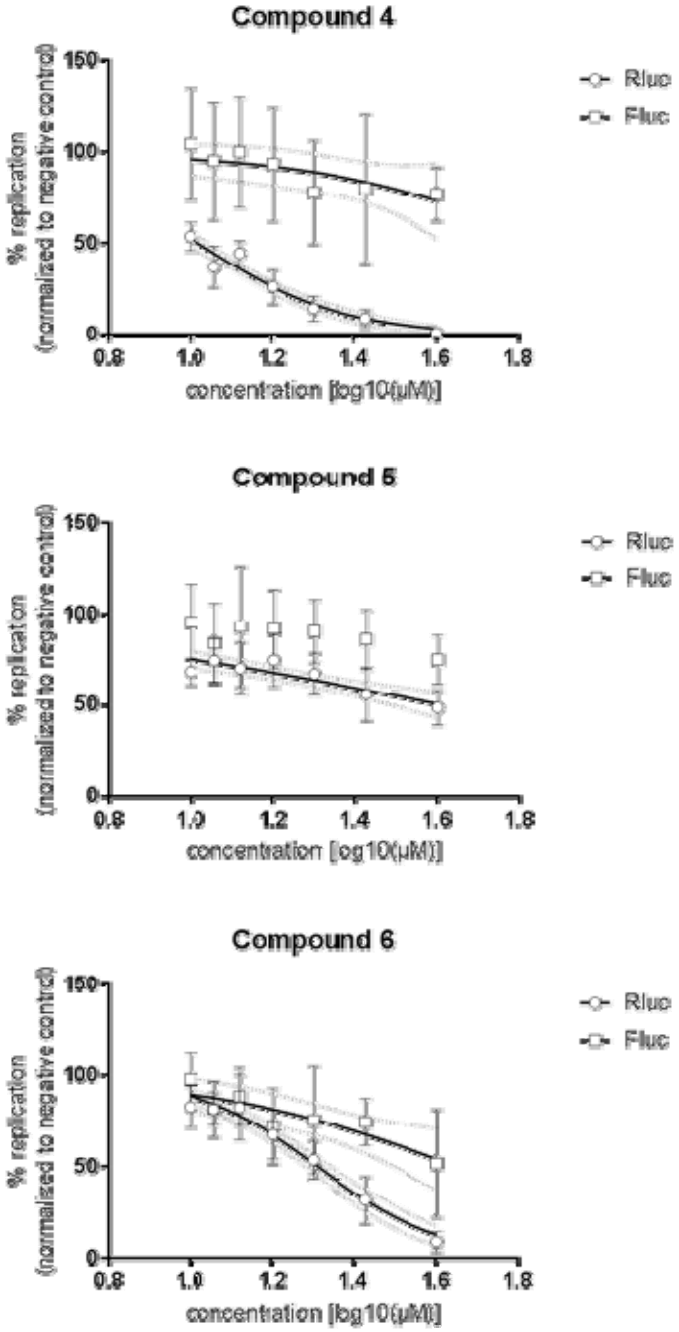

Fig. 5. Comparison of antiviral activities of compounds **4**-**6** from *Cytospora* sp. in different concentrations.

Table 1
^{13}C and ^{1}H NMR spectroscopic data of compounds **1** and **2** in methanol-d_4

Position	**1**		**2**	
	δ_C, Type	**δ_H (*J* in Hz)**	**δ_C, Type**	**δ_H (*J* in Hz)**
1	176.1, C	/	175.9, C	/
2	72.5, CH	4.82 d (6.7)	74.0, CH	4.62 d (8.2)
3	62.7, CH	4.20 brd (6.7)	63.1, CH	4.20 d (8.2)
4	209.1, C	/	208.5, C	/
5	37.7, CH_2	2.69–2.76 m	38.7, CH_2	2.74–2.79 m
6	28.9, CH_2	2.44–2.48 m	28.8, CH_2	2.45–2.49 m
7	176.4, C	/	176.3, C	/
1′	136.2, C	/	136.0, C	/
2′	131.2, CH	7.32–7.34 m	131.2, CH	7.31–7.33 m
3′	129.7, CH	7.32–7.34 m	129.7, CH	7.31–7.33 m
4′	128.9, CH	7.32–7.34 m	128.9, CH	7.31–7.33 m
5′	129.7, CH	7.32–7.34 m	129.7, CH	7.31–7.33 m
6′	131.2, CH	7.32–7.34 m	131.2, CH	7.31–7.33 m

Table 2
^{13}C and ^{1}H NMR spectroscopic data of compound **3** in acetone-d_6

Position	**δ_C, Type**	**δ_H (*J* in Hz)**	**Position**	**δ_C, Type**	**δ_H (*J* in Hz)**
1	180.3, C	/	1′	123.5, C	/
2	153.3, C	/	2′	133.3, CH	7.41 d (8.9)
3	118.8, C	/	3′	114.6, CH	6.98 d (8.9)
4	177.5, C	/	4′	159.7, C	/
4a	153.5, C	/	5′	114.6, CH	6.98 d (8.9)
5a	152.3, C	/	6′	133.3, CH	7.41 d (8.9)
6	99.6, CH	7.22 s	1″	65.4, CH_2	4.60 d (6.5)
7	149.2, C	/	2″	121.2, CH	5.49 m
8	146.7, C	/	3″	137.9, C	/
9	106.4, CH	7.44 s	4″	18.3, CH_3	1.76 brs
9a	114.9, C	/	5″	25.9, CH_3	1.78 brs
9b	119.8, C	/			

Table 3
^{13}C and ^{1}H NMR spectroscopic data of compounds **4**–**6** in acetone-d_6

Position	**4**		**5**		**6**	
	δ_C, Type	δ_H (*J* in Hz)	δ_C, Type	δ_H (*J* in Hz)	δ_C, Type	δ_H (*J* in Hz)
2	116.2, C	/	116.2, C	/	114.7, C	/
5	115.6, C	/	115.7, C	/	114.3, C	/
1'	121.8, C	/	122.6, C	/	121.7, C	/
2'	111,0, CH	6.65 s	118.8, CH	7.08 brs	131.9, CH	7.42 d (8.7)
3'	145.7, C	/	145.1, C	/	114.3, CH	6.88 d (8.7)
4'	133.8, C	/	146.0, C	/	156.9, C	/
5'	145.7, C	/	115.5, CH	6.87 d (8.2)	114.3, CH	6.88 d (8.7)
6'	111.0, CH	6.65 s	123.8, CH	6.93 brd (8.2)	131.9, CH	7.42 d (8.7)
1″	123.3, C	/	122.2, C	/	122.8, C	/
2″	132.8, CH	7.47 d (8.9)	132.8, CH	7.47 d (8.4)	131.7, CH	7.50 d (8.8)
3″	114.7, CH	6.97 d (8.9)	114.7, CH	6.98 d (8.4)	113.7, CH	6.96 d (8.8)
4″	159.6, C	/	159.6, C	/	158.5, C	/
5″	114.7, CH	6.97 d (8.9)	114.7, CH	6.98 d (8.4)	113.7, CH	6.96 d (8.8)
6″	132.8, CH	7.47 d (8.9)	132.8, CH	7.47 d (8.4)	131.7, CH	7.50 d (8.8)
1‴	65.4, CH_2	4.60 d (6.6)	65.4, CH_2	4.60 d (6.5)	64.5, CH_2	4.60 d (6.5)
2‴	121.2, CH	5.49 m	121.2, CH	5.49 m	120.3, CH	5.49 m
3‴	137.9, C	/	137.9, C	/	136.9, C	/
4‴	18.3, CH_3	1.76 brs	18.3, CH_3	1.76 brs	17.3, CH_3	1.76 brs
5‴	25.9, CH_3	1.78 brs	25.9, CH_3	1.78 brs	24.9, CH_3	1.78 brs

Table 4
MIC values (µg/mL) against the tested microorganisms.

Organism	MIC (µg/ml)											
	1	**2**	**3**	**4**	**5**	**6**	**7**	**8**	**9**	**10**	**11**	Reference
Candida albicans DSM 1665	.n.i	.n.i	.n.i	66.66	.n.i	66.66	.n.i	.n.i	.n.i	.n.i	.n.i	N 33.33
Micrococcus luteus DSM 1790	.n.i	.n.i	66.66	16.66	33.33	33.33	.n.i	.n.i	.n.i	.n.i	.n.i	O 0.41
Mucor hiemalis DSM 2656	66.66	66.66	66.66	33.33	33.33	33.33	66.66	66.66	66.66	66.66	.n.i	N 16.66
Pichia anomala DSM 6766	.n.i	.n.i	.n.i	.n.i	.n.i	.n.i	.n.i	.n.i	.n.i	.n.i	.n.i	N 16.66
Rhodoturula glutinis DSM 10134	.n.i	66.66	33.33	33.33	66.66	33.33	66.66	.n.i	66.66	66.66	66.66	N 4.16
Schizosaccharomyces pombe DSM 70572	.n.i	.n.i	.n.i	.n.i	.n.i	.n.i	.n.i	.n.i	.n.i	.n.i	.n.i	N 16.66
Bacillus subtilis DSM 10	.n.i	.n.i	66.66	66.66	66.66	66.66	.n.i	.n.i	.n.i	.n.i	.n.i	O 8.33
Chromobacterium violaceum DSM 30191	.n.i	.n.i	66.66	33.33	66.66	66.66	.n.i	.n.i	.n.i	66.66	.n.i	O 0.41
Escherichia coli DSM 1116	.n.i	.n.i	.n.i	.n.i	.n.i	66.66	.n.i	.n.i	.n.i	.n.i	.n.i	O 1.66
Mycobacterium smegmatis DSM ATCC 700084	.n.i	.n.i	.n.i	.n.i	.n.i	.n.i	.n.i	.n.i	.n.i	.n.i	.n.i	K 0.83
Pseudomonas aeruginosa DSM PA14	.n.i	.n.i	.n.i	.n.i	.n.i	.n.i	.n.i	.n.i	.n.i	.n.i	.n.i	G 0.41
Staphylococcus aureus DSM 346	.n.i	.n.i	33.33	16.66	16.66	16.66	.n.i	.n.i	.n.i	.n.i	.n.i	O 0.41

ni: no inhibition, N: Nystatin, O: Oxytetracyclin, K: Kanamycin, G: Gentamycin.

Table 5
Cytotoxicity (IC_{50}) against two different cell lines.

Cell line	IC50 μg/ml											
	1	**2**	**3**	**4**	**5**	**6**	**7**	**8**	**9**	**10**	**11**	Epothilon B
L929	.n.a	.n.a	26	7.8	7	19	.n.a	.n.a	.n.a	5.8	.n.a	0.00038
KB3.1	.n.a	.n.a	17	5.9	6.5	5	.n.a	.n.a	.n.a	2.4	.n.a	0.000027

Table 6

Biofilm and Preformed Biofilm Inhibition Activity.

Conc. (µg/ml)	Assay	Biofilm and Pre-biofilm inhibition %										
		1	**2**	**3**	**4**	**5**	**6**	**7**	**8**	**9**	**10**	**11**
	MIC (µg/ml)	no*	no	32	16	16	16	no	no	no	64	64
256	Biofilm	74.14	72.68	85.27	83.16	85.1	86.92	85.9	77.8	89.5	85.62	85.29
	Pre-biofilm	na**	na	na	na	na	68.05	na	na	na	na	na
128	Biofilm	48.40	65.64	83.78	78.91	85.1	86.75	80.18	35.91	82.45	81.49	81.08
	Pre-biofilm	na	na	na	na	na	60.75	na	na	na	na	na
64	Biofilm	53.68	29.77	32.92	12.58	85.6	85.14	65.05	13.41	42.86	75.31	76.3
	Pre-biofilm	na	na	na	na	na	51.86	na	na	na	na	na
32	Biofilm	12.3	na	na	na	61.12	84.73	60.1	2.52	14.66	27.85	na
	Pre-biofilm	na	na	na	na	na	na	na	na	na	na	na
16	Biofilm	na	na	na	na	34.42	73.30	55.96	na	na	4.44	na
	Pre-biofilm	na	na	na	na	na	na	na	na	na	na	na
8	Biofilm	na	na	na	na	na	42.16	41.18	na	na	na	na
	Pre-biofilm	na	na	na	na	na	na	na	na	na	na	na
4	Biofilm	na	na	na	na	na	30.94	40.60	na	na	na	na
	Pre-biofilm	na	na	na	na	na	na	na	na	na	na	na

*no: not obtained, **na: not active